

Article

Mechanical Characteristics of an Open-Buried Double-Arch Tunnel during Construction

Yu-Liang Lin *, Ya-Lin Guo, Guo-Lin Yang and Pei-Ran Zhang

School of Civil Engineering, Central South University, Changsha 410075, China; guoyalin1997csu@163.com (Y.-L.G.); yangguolin6301@163.com (G.-L.Y.); zhangpr91@163.com (P.-R.Z.)
* Correspondence: linyuliang11@163.com

Abstract: The open excavation and concealed construction method is widely adopted for the construction of bias double-arch tunnels. However, the mechanical behavior of the tunnel during the whole construction period by using the open excavation and concealed construction method is not well understood, and the basis for construction organization and optimization is lacking. Based on an open-buried double-arch tunnel on Xiajuan Road, Changsha City, China, on-site monitoring was carried out in terms of the deformation of the steel arch in the primary lining, the stress of reinforcement in the secondary lining, and the deformation of the surrounding rock during the construction process. The correlation between the vault settlement rate and the steel arch strain was analyzed. The results show that the maximum vault settlement and settling rate of the left and right caverns occur at different locations due to different supporting conditions. The peripheral displacement experiences a process of convergence inward and extension outward. The compressive steel stress in the secondary lining of the right cavern is greater than that in the left cavern, except for the points at the arch waist. The backfill above the left cavern reduces the loading on the lining of the right cavern, but it increases the loading on the left cavern. The bias effect of the open-buried double-arch tunnel is well controlled and balanced when the open excavation and concealed construction method is adopted.

Keywords: open-buried double-arch tunnel; bias pressure; supporting structure; surrounding rock deformation; mechanical characteristics; on-site monitoring



Citation: Lin, Y.-L.; Guo, Y.-L.; Yang, G.-L.; Zhang, P.-R. Mechanical Characteristics of an Open-Buried Double-Arch Tunnel during Construction. *Appl. Sci.* **2023**, *13*, 3891. <https://doi.org/10.3390/app13063891>

Academic Editor: Daniel Dias

Received: 1 March 2023

Revised: 15 March 2023

Accepted: 17 March 2023

Published: 18 March 2023



Copyright: © 2023 by the authors. Licensee MDPI, Basel, Switzerland. This article is an open access article distributed under the terms and conditions of the Creative Commons Attribution (CC BY) license (<https://creativecommons.org/licenses/by/4.0/>).

1. Introduction

Because of its advantages of a smooth alignment, a small footprint, and excellent space utilization, the double-arch tunnel becomes one of most widely used types of tunnel structures, and it is frequently employed in highway engineering. Thus, the mechanical behavior of the tunnel is regarded by many scholars in terms of the deformation laws of the tunnel lining and surrounding rock, as well as the control measures to restrain the deformation of the tunnel and surrounding rock [1–4].

Generally, the engineering behaviors of different geotechnical structures can be well reflected by numerical simulation [5–7] and experimental investigation [8–10]. Zhao et al. [11] investigated the deformation characteristics of the crossing section of two municipal tunnels subjected to construction load by on-site experiments. Chang et al. [12] investigated the behavior of a tunnel caused by adjacent excavation and established a reference for excavation standard. Sharma et al. [13] discussed the influence of the stiffness of tunnel lining on the displacement and distortion by on-site investigation. Fahimifar et al. [14] predicted the deformation of the surrounding rock around the tunnel based on different calculation models or methods.

The construction method for the double-arch tunnel includes the double-side-drift method, the CD method, the benching method, and the CRD method [15,16]. The different methods are suited for different engineering geological conditions, and the suitability of different methods for the construction tunnels has been discussed by many scholars [17–21].

Dong et al. [22] studied the construction techniques of the entrance of an urban double-arch tunnel to improve the construction efficiency and ensure the stability of the tunnel entrance section. Cai [23] optimized the distribution of the stress release ratio to determine the proper installation time for the secondary liner. Considering the skewed distribution characteristics, Li et al. [24] built a computational model of a double-arch tunnel to analyze the pressure evolution of the surrounding rock during step-by-step excavation of a double-arch tunnel. Li et al. [25] presented analytical solutions for internal forces of a lining structure in a shallow double-arched tunnel subjected to unsymmetrical loading.

The deformation mode of the arch structures of the tunnel can be determined based on the curved beam theory, and a more accurate inversion analysis scheme can be proposed [26]. However, in engineering practice, the tunnel is generally constructed under a sloping mountain, which subsequently results in different burial depths for different caverns. An open-buried double-arch bias tunnel structure system is no longer compatible with the concealed excavation method for excavation [27]. Lai [28] described the design and calculation of a large-span open-buried double-arch tunnel from the aspect of engineering design. Hu et al. [29] adopted finite element software to analyze the stress distribution and displacement characteristics of surrounding rock and linings in two types of open-buried tunnel structures, half-road and half-tunnel, subjected to different construction conditions.

The existing literature has greatly developed the construction technology of tunnels. However, due to the constraints of the terrain and the complexity of the construction process, the varied open-buried double-arch tunnels with different section forms show different engineering mechanical behaviors. In this study, based on an open-buried double-arch tunnel on Xiajuan Road, Changsha city, China, the evolution of the deformation of the surrounding rock and the mechanical properties of the supporting structure of the open-buried double-arch tunnel subjected to construction load are studied. The study aims to provide a basis for the optimization of the supporting structure and a guideline for the construction plan of the tunnel, as well as a reference for the design and construction of related tunnels.

2. Project Summary

2.1. Tunnel on Xiajuan Road

The double-arch municipal tunnel with a two-way four-lane structure is located on Xiajuan Road, Changsha City, China. The mileage range of the tunnel is K2 + 060~K2 + 380 with a total length of 320 m, and the concealed section is about 280 m in length. The width and the height of tunnel structure are 14.75 m and 5.5 m, respectively. The cross-section area of internal profile of a single tunnel cave is 154.39 m². The tunnel is oriented from north to south, and the overall topography of construction site shows a high elevation in the south and a low elevation in the north. The inlet and the cave section are high in the west and low in the east. A composite tunnel lining is adopted according to the principle of NATM, in which the primary lining adopts a 15 × 15 bar-mat reinforcement of Φ8, I22b steel arch and C25 shotcrete, and the secondary lining is supported by molded reinforced concrete with a thickness of 70 cm.

2.2. Engineering Geological Condition

The stratigraphic distribution in construction site mainly includes Plant layer, Quaternary sedimentary layer, Quaternary relict deposits, and underlying bedrock. The underlying bedrock is paleoproterozoic muddy and sandy slate. The lithological characteristics of stratigraphic layer are described in Table 1. The location, longitudinal and cross profiles, and geological conditions of the tunnel project are shown in Figure 1.

Table 1. Summary of stratigraphic lithology characteristics.

Number	Stratigraphic Types	Characteristic Description
①	Plant layer	This layer is brown, tawny, and mainly composed of clayey soil interspersed with plant roots and mixed with a small amount of gravel in a slightly wet and loose state, which is mainly distributed on the surface of the mountain. The thickness of this layer is in the range of 0.1~0.30 m.
②	Quaternary freshly deposited silt	This layer is grey-black, with a wet-saturated and flow plastic state. Its dry strength and toughness are low, with a layer thickness of <3.00 m.
③	Quaternary residual deposit silty clay	This layer is brownish-yellow or reddish-brown, locally interspersed with weathered rock blocks that have not weathered completely. It is in a slightly wet, hard plastic state and its dry strength and toughness are medium. Its layer thickness is 0.50–7.60 m, and its average thickness is 2.25 m.
④	Paleoproterozoic slate	Within the exploration depth, this layer can be divided into muddy slate and sandy slate according to its mineral composition.

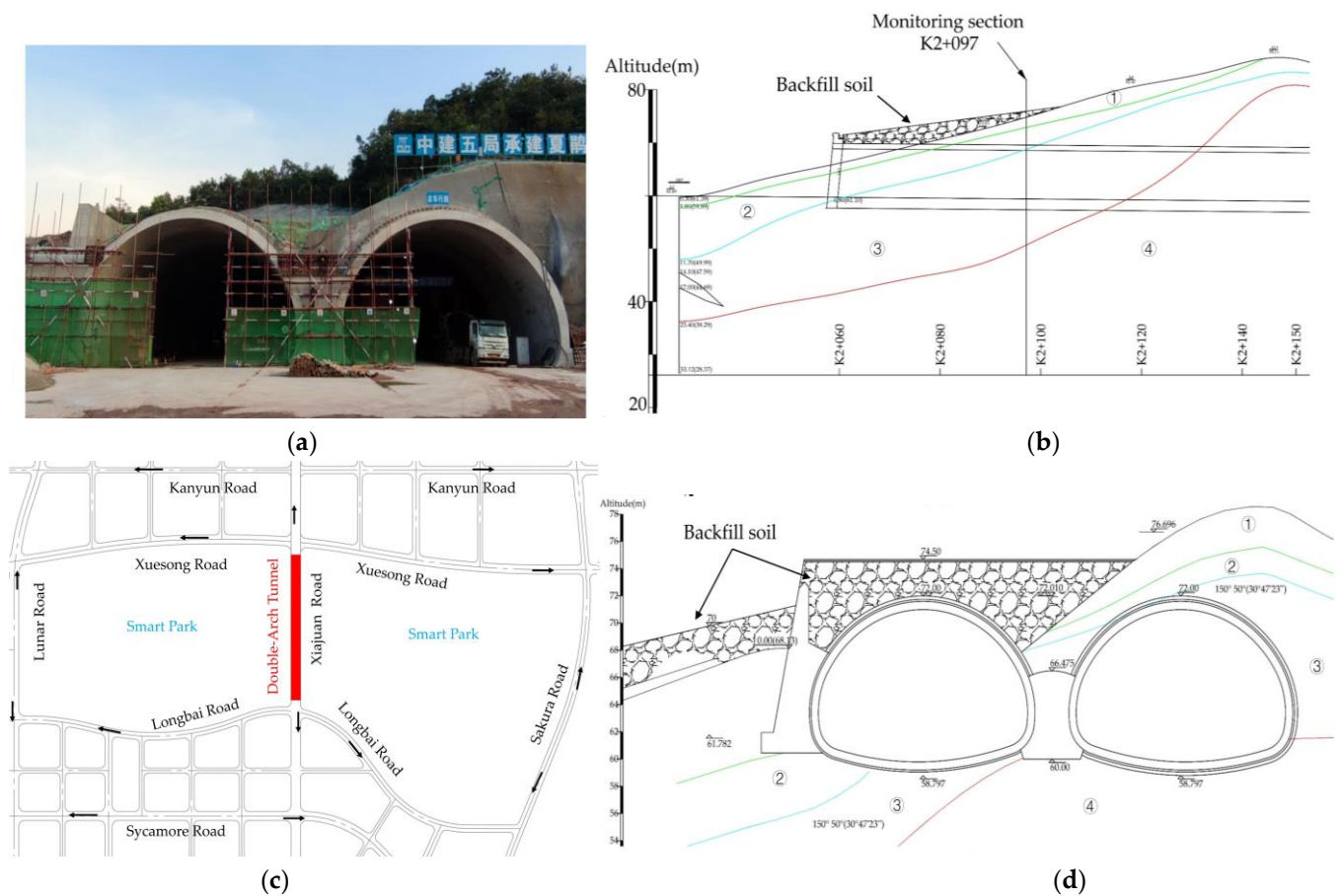


Figure 1. Location and longitudinal and cross profiles of the double-arch tunnel on Xiajuan Road. (a) Front view of tunnel; (b) Longitudinal geological profile; (c) Project location map; (d) Monitoring section K2 + 097.

The cavern section is surrounded by soil, strongly weathered rock layers, and medium weathered rock layers, with large differences in rock hardness and integrity. Consequently, the grade of the surrounding rock is determined as V.

2.3. Construction Process of the Tunnel Entrance

The tunnel entrance section of Xiajuan Road in Changsha City, China (mileage range K2 + 060~K2 + 100) shows a great difference in burial depth between the two sides of the cavern. The left cavern is very shallow, with more than 1/2 of the cavern exposed to

the surface, while the right cavern is located inside the mountain (burial depth of 2~6 m), forming a distinctive open-buried double-arch tunnel. Because of a serious topographic deviation in this section, a deflecting retaining wall was added on the left side of the left cavern to prevent tunnel instability or other disasters during the tunnel construction and service period. When the linings in both caverns were completed, soil backfill was performed above the left cavern to balance the topographic deviation of the mountain. The left cavern of the entrance section adopted an open excavation and a concealed construction method. Before the initial support of the left cavern, the excavated soil from other places was back-filled into the left cavern, so as to establish the up-step steel arch. The right cavern was constructed by the concealed excavation method. Both the left and the right caverns were excavated using the three-step ring-cut method. The left and right caverns were constructed in order, keeping the staggered distance of the cavern palm surface more than twice that of the tunnel span, and the longitudinal distance of the upper and lower steps should be less than 5 m. Meanwhile, the longitudinal distance of each cavern was adjusted in time according to the monitoring results. To make the construction process clear, Figure 2 shows the construction schedule in detail, and the corresponding construction is shown in Table 2.

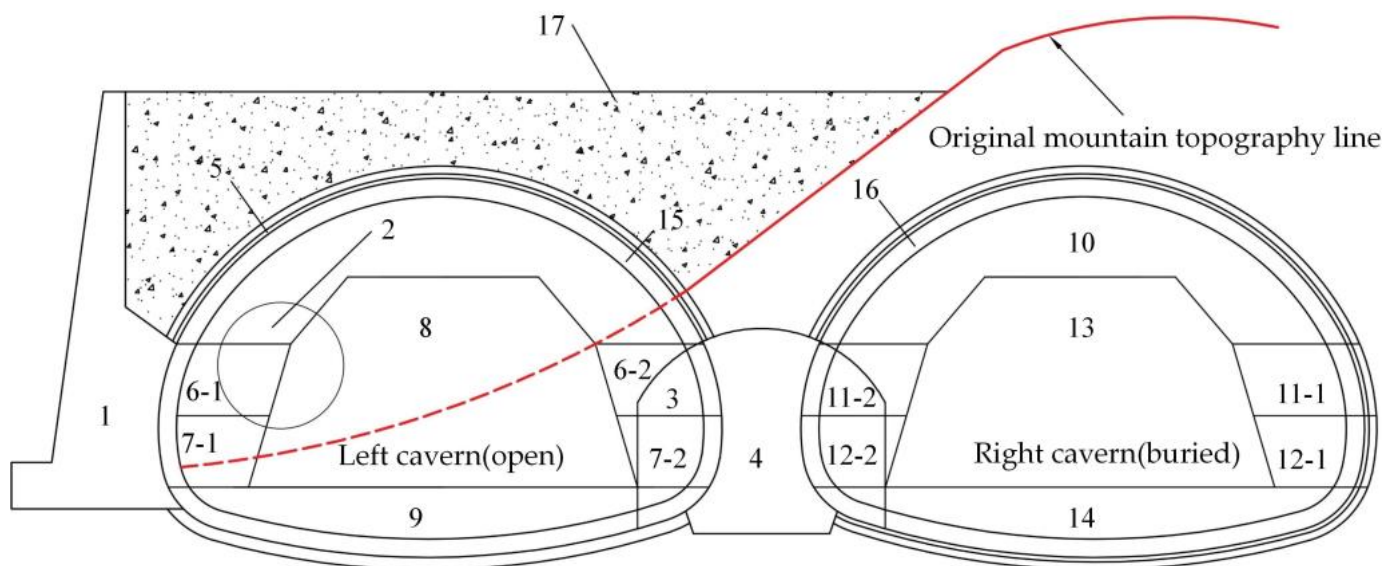


Figure 2. Schematic diagram of the construction process of the open-buried double-arch and bias tunnel.

3. On-Site Monitoring Program

3.1. Monitoring Objects and Content

According to the condition of construction site, a typical monitoring section is selected at the mileage of K2 + 097. The stress and strain of the supporting structure are investigated, including the strain of steel arch in primary lining, the stress of rebar and the strain of concrete in secondary lining. Meanwhile, the deformation of the surrounding rock is also observed, including the vault settlement and the tunnel perimeter convergence. The layout of measurement points and the point number at the tunnel cross-section are shown in Table 3 and Figure 3.

Table 2. The main construction and its construction sequence.

Number	Corresponding Construction	Number	Corresponding Construction	Number	Corresponding Construction
1	Deflecting retaining wall construction	7	Lower-step excavation in the left cavern	13	Excavation of the core soil in the right cavern
2	Soil backfill in the left cavern	8	Excavation of the core soil in the left cavern	14	Soil excavation and primary lining and invert construction in the right cavern
3	Central guide excavation and temporary steel arch support	9	Soil excavation and primary lining and invert construction in the left cavern		
4	Mid-partition wall construction	10	Up-step excavation and primary lining in the right cavern	15	Construction of the secondary lining in the left cavern
5	Erection of the up-step in the left cavern	11	Mid-step excavation in the right cavern and primary lining construction	16	Construction of the secondary lining of the right cavern
6	Mid-step excavation in the left cavern	12	Excavation and primary lining of the lower step in the right cavern	17	Soil backfill in the left cavern

Table 3. List of monitoring contents and location of measurement points.

Item	Instruments	Location and Number of Measurement Points
Steel arch strain	Strain gauges	Left arch waist—LW, Left arch shoulder—LS, Vault—V, Right arch shoulder—RS, Right arch waist—RW
Concrete strain	Strain gauges	Left arch foot—LF, Left arch waist—LW, Vault—V, Right arch waist—RW, Right arch foot—RF
Reinforcement stress	Stress gauges	Left arch foot—LF, Left arch waist—LW, Vault—V, Right arch waist—RW, Right arch foot—RF
Vault settlement	Precision level+ Micrometer	Left measurement point—LM, Vault measurement point—VM, Right measurement point—RM
Perimeter convergence	Digital convergence meter	Upper horizontal line—UH, Lower horizontal line—LH

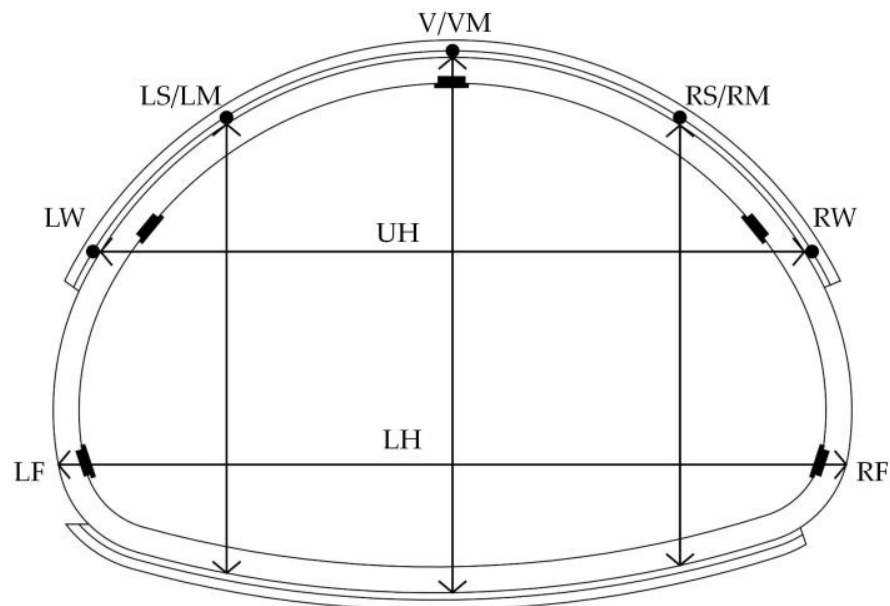


Figure 3. Measurement point layout.

3.2. Component Arrangements

According to existing reports [30–32], the measurement of stress or strain at the steel arch was mostly conducted by arranging steel stress gauges or strain gauges parallel to the inner and outer flange sides of the steel arch. Thereafter, the test results were converted into axial force or bending moment of the steel arch, and then the internal force of the steel arch could be analyzed. There were few experimental results related to the force or deformation investigation in any abdominal region of the steel arch. If the strain gauges are arranged on inner and outer flanges of the steel arch in parallel, the changing trend of the contact pressure between the liners cannot be reflected sensitively. The strain gauge arrangement on the web axis of the steel arch can not only reflect the deformation of the steel arch effectively, but also indirectly reflect the changing trend of the contact pressure between the liners.

A fixing device was utilized to weld the strain gauge to the center of web along the axis of steel arch, and a protective shell was welded to steel arch to ensure that the strain gauge would not be damaged during the shotcrete process, as shown in Figure 4. The stress gauge was welded to the reinforcement of secondary lining in the direction of tunnel circumference to measure the main circumferential axial force of reinforcement. The strain gauges were fixed to the reinforcement of secondary lining by using ties at both ends to measure the strain of the second liner concrete. The vault settlement was measured by a micrometer with a high precision. The tunnel perimeter convergence was measured by a digital convergence meter.

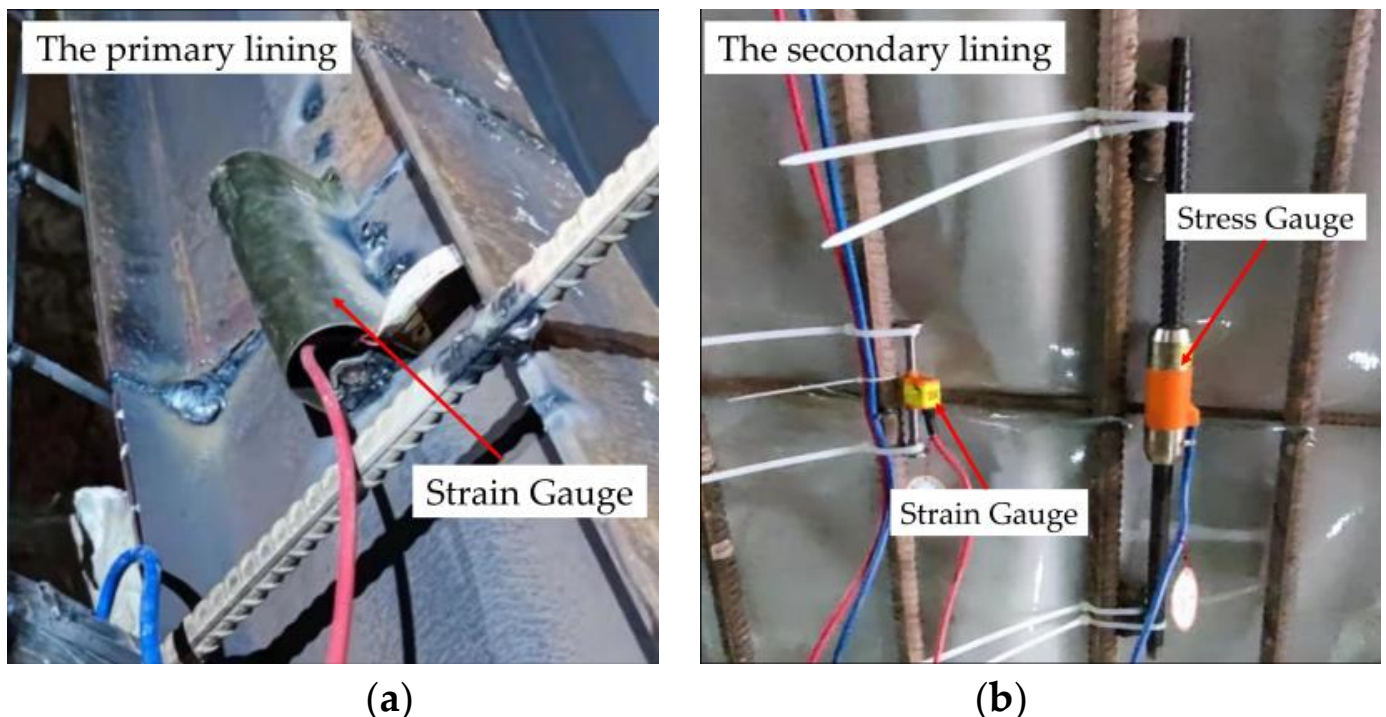


Figure 4. Diagram of field components installation: (a) Strain gauge installation in primary lining; (b) the strain gauge and stress gauge installation in secondary lining.

3.3. Construction Cases

The on-site test data were collected corresponding to the construction progress until stability was achieved. More than 240 days were spent on this on-site monitoring. To more clearly illustrate the force and the deformation evolution of the supporting structure and surrounding rock during the construction, the construction cases were numbered according to the construction sequence and time, as shown in Table 4. There are mainly

nine construction cases which are numbered as Cases ①~⑨, and four construction stages marked by Stages I~IV.

Table 4. Main construction cases and construction stages.

Construction Stage	Construction Case	Specific Construction	Construction Time
I	①	Excavation and erection of up-step in the left cavern	24 Marh
	②	Excavation and erection of mid-step in the left cavern	19 April
	③	Construction of the invert in the left cavern	6 May
II	④	Excavation and erection of up-step in the right cavern	30 April
	⑤	Construction of the invert in the right cavern	30 May
III	⑥	Construction of the secondary lining in the left cavern	21 July
	⑦	Construction of the secondary lining in the right cavern	10 August
IV	⑧	The beginning of soil backfills	26 August
	⑨	The ending of soil backfills	5 October

4. On-Site Test Results and Analysis

4.1. Steel Arch Strain

Figure 5 shows the strain–time distribution of the steel arch in the monitoring section of the tunnel, in which tension strain is represented by a positive value, and compression strain is marked by a negative value. The strain is assumed as zero when the upper steel arch is erected along the upper step. Combined with the arrangement of the measurement points in the tunnel section (see Table 3 and Figure 3) and the division of the construction cases (see Table 4), the variation of the strain at the steel arch is analyzed corresponding to different construction stages, as follows.

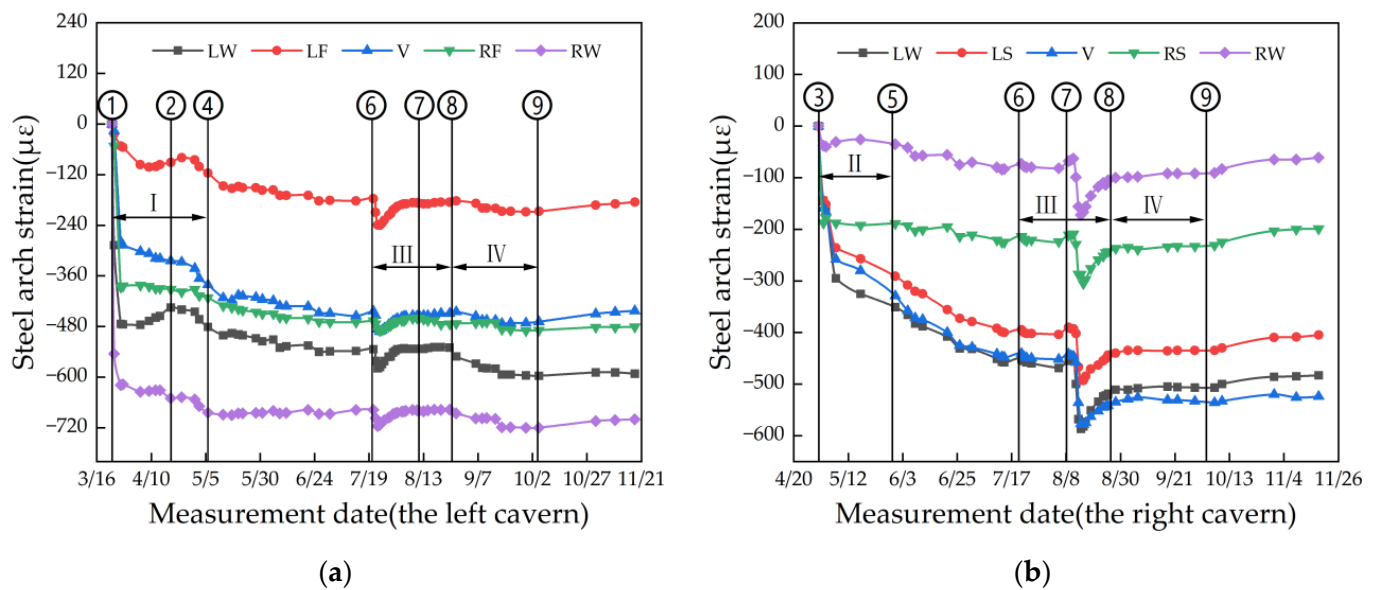


Figure 5. Strain distribution of the steel arch versus time. (a) Left cavern; (b) right cavern.

- (1) Construction stage I. The up-step of the left tunnel is located above the original hillside surface. Consequently, after the construction of the deflecting retaining wall, the primary lining at the up-step of the left tunnel is constructed (as shown in Figure 2). It is seen that after the completion of the primary lining, the strain at the steel arch shows a rapid growth trend at the early stage due to the effect of the concrete, formwork, and its own gravity. The strain development at each portion of the steel arch gradually flattens out with time. It is worth noting that the strain at the remaining measurement point continues to increase while the strain at the LW and the LS of the steel arch decreases because the right side of the steel arch that

overlaps with the mid-partition wall shares part of the right side of the surrounding rock pressure. However, when the mid-step of the left cavern is excavated, the strain at the LW and the LS increases simultaneously, and the increasing trend is smaller than at other positions. This indicates that the soil displacement of the middle-lower parts of both sides of the left cavern are caused by the excavation of the mid-step, driving a stress adjustment of the surrounding rock and squeezing the steel arch to a certain extent. Under the deflecting effect of right hillside body, the mid-partition wall on the right side shows a tendency to deflect to the left cavern after the removal of surrounding rock at the left side. Consequently, the pulling and squeezing effect at the steel arch on the same side is more obvious. During the construction of the lower step of the cavern, the above phenomenon becomes more obvious, and the strain growth increases significantly. It is seen that after the construction of the open cavern by the concealed method, the primary lining plays a certain role in the supporting action, especially for the hillside body on the mid-partition wall. In summary, regarding the construction of the open-buried double-arch tunnel, although the influence of the traditional (buried tunnel) up-step excavation on the tunnel supporting system and surrounding rock can be ignored, the soil excavation of the middle-lower part of the open cavern, which is equivalent to the unloading of the slope angle, has induced a stress adjustment of the rock around the left cavern and an attitude change of the mid-partition wall. It is necessary to adopt engineering measures (e.g., installing the deflecting retaining wall) to improve the stability of the whole tunnel and slope subjected to the open cavern construction load.

- (2) Construction stage II. After the excavation and erection of the primary lining at the up-step of the right cavern, the surrounding rock pressure is released within 3 days. The steel arch strain increases rapidly when it begins to bear the surrounding rock pressure. As the up-step of the right cavern continues to be excavated, the strain of the steel arch at the RW and the RS is essentially stable, while the other points continue to increase until the construction of the invert begins. The reason for the above phenomenon is that the right side of the right cavern is on a higher elevation of mountain topography, while the left side is reduced in height and linked with the mid-partition wall. The caverns are in a right-to-left skewed topography. After the excavation of the up-step and the invert in the right cavern, the surrounding rock deforms towards the left side with a stress adjustment, and the left side of the steel arch bears the surrounding rock pressure. It is seen that the location of the joint area (near the mid-partition wall) is a sensitive area during the buried-cavern construction of the open-buried double-arch tunnel.
- (3) Construction stage III. The strain at the steel arch increases rapidly in both caverns within 3 days after the secondary lining is applied, and reaches the maximum value during the monitoring period. After 5 days, the strain at the steel arch of the left and right caverns decreases rapidly until they are essentially stable. The reason for the above phenomenon is that contact pressure arises between the primary and the secondary linings due to gravity and the solidification of the concrete when the secondary lining is completed [33]. While the secondary-lining trolley is still acting on the secondary lining, the contact pressure between the linings causes the strain at the steel arch to increase rapidly. When the secondary-lining trolley is removed, there is a certain release of interaction force between the linings. Meanwhile, the secondary lining concrete at this time tends to be stable due to its solidification. It is worth noting that the strain of the steel arch at each measurement point of the right cavern did not increase repeatedly due to the soil excavation when the secondary lining of the left cavern was completed. The strain tends to be stable after it slightly decreases during the construction of the secondary lining of the right cavern. It is seen that the supporting strength at the open cavern side in the open-buried double-arch tunnel is effectively utilized, which is of great significance to guarantee the stability of the tunnel structure system.

- (4) Construction stage IV. When the secondary linings of the left and right caverns reach the design strength, the soil is back-filled on the left cavern (open cavern). It is seen that the backfill presents different effects on the strain at the steel arch in both caverns. Soil backfill increases the strain at the steel arch of the left cavern again, which is especially significant at the LW, while the strain at the steel arch of the right cavern decreases at the end of backfill. Soil backfill will increase the surrounding rock pressure around the left cavern, which indicates that it causes a transformation from an “open” cavern into a “buried” cavern. The bias pressure caused by the slope is balanced, which subsequently reduces the strain at the steel arch of the right cavern, and increases the strain at the left cavern. During the whole process, the strain at each measurement point is still within the safe range.

4.2. Vault Settlement

The vault settlement was continuously monitored after the steel arch support at the up-step was established in the left and right caverns. The value of the vault settlement and its sinking rate are shown in Figure 6.

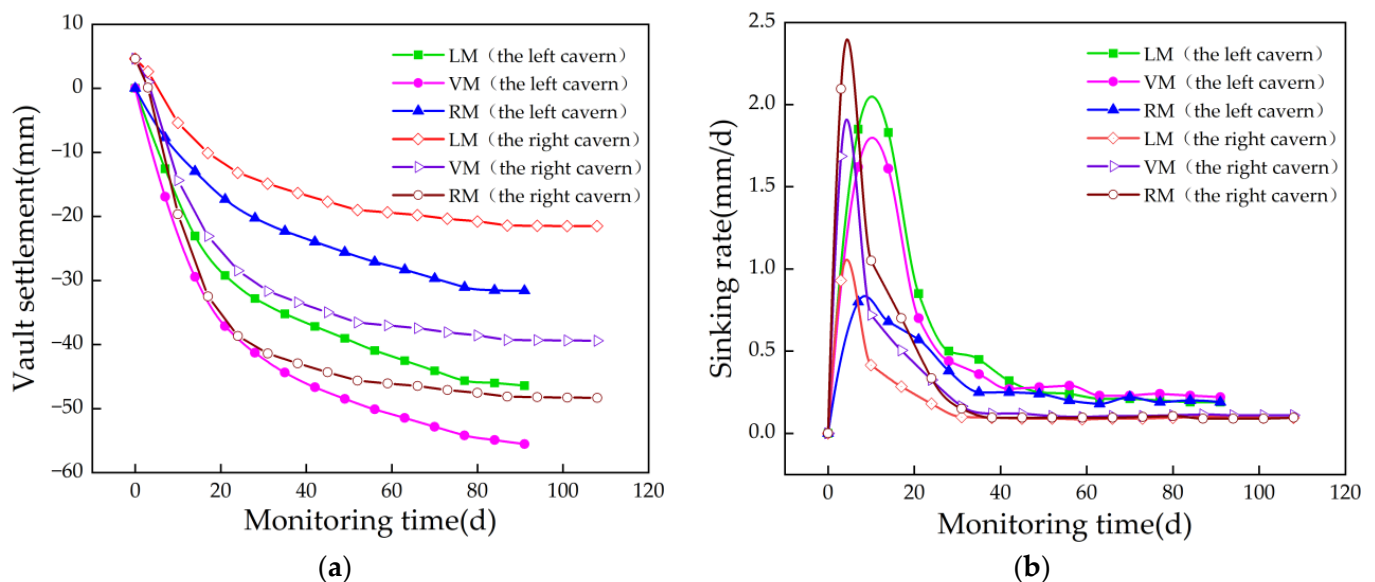


Figure 6. Development of the settlement and sinking rate of the vault. (a) Vault settlement; (b) the sinking rate of vault settlement.

- (1) The process of vault settlement can be divided into three stages: the rapid development stage within 15 d after the construction of up-step, the continuous development stage before the application of the invert, and the gradual stabilization stage after the application of the invert. The vault settlement at each stage accounts for about 50%, 30%, and 20% of the total settlement. After the application of the invert, the sinking rate gradually tends to be stable.
- (2) The stabilization periods of vault settlement in the left and right caverns are different. It takes 42 d and 30 d for vault settlement of the left and right caverns to reach stability, respectively. At the section of 30.5 m to working face, the settlement value of the vault at the left cavern reaches about 80% of the total settlement. This result is consistent with the observation of Yuan et al. [34]. Since this study relies on an open-buried double-arch tunnel, there is no surrounding rock above the open cavern. This prompts the time for the vault settlement to reach stability, and reduces the distance from the working face between the former cavern and the later cavern.
- (3) The maximum vault settlement position and the sinking rate in each cavern are different. The maximum vault settlement and sinking rate of the left cavern occur at

the VM, while they occur at the RM in the right cavern. The minimum settlement and sinking rates of each cavern occur in the measurement point near the mid-partition wall. The reason is that the deflecting retaining wall and the mid-partition wall effectively suppress the overall sinking of the primary lining at the measurement points. The maximum vault settlement of the left and right caverns is 55.5 mm and 49.0 mm, respectively, which are about 1/3 of the admissible value (150 mm). The open-excavation and concealed construction method is effective to control the settlement of the tunnel during the construction of the tunnel.

4.3. Peripheral Displacement

Peripheral displacement refers to the displacement of measurement points in surrounding rock within the tunnel boundary after excavation. It is difficult to accurately measure the absolute value of displacement of spatial points. Consequently, it is common to determine the relative displacement of two points along the direction of inner wall of the tunnel. The peripheral displacement of the surrounding rock of the tunnel is reflected by monitoring the relative displacement of the points along the upper and lower horizontal lines. The peripheral displacement vs. time on the left and right caverns of the tunnel is shown in Figure 7, in which the negative value indicates an inward convergence, and the positive value refers to an outward extension deformation. The positions of the upper horizontal line (UH) and the lower horizontal line (LH) are shown in Table 3 and Figure 3.

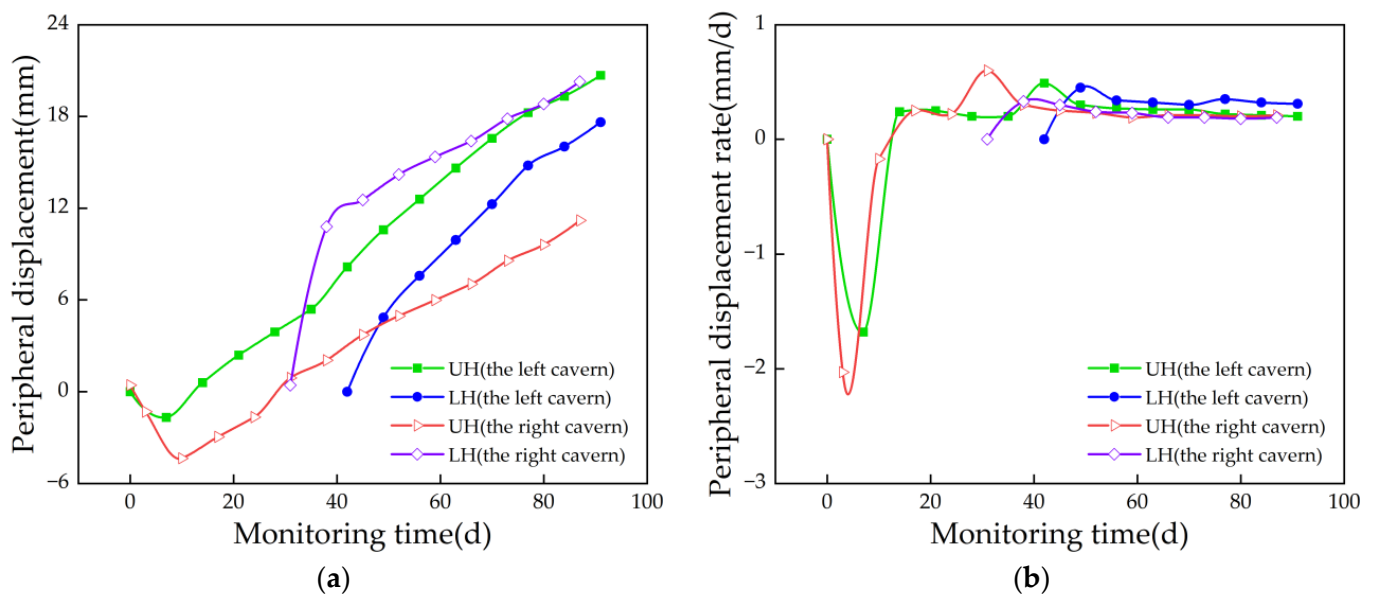


Figure 7. Peripheral displacement and displacement rate versus time. (a) Peripheral displacement; (b) peripheral displacement rate.

- (1) The peripheral displacement around the tunnel shows an inward convergence, and then experiences an outward extension. After the construction of the up-step of the tunnel, the peripheral displacement of the left and right caverns tends to move inwards. The main reason for this phenomenon is that the mid-partition wall moves towards the shallowly buried side (left cavern) subjected to the deflection of slope. Regarding the right cavern, after the construction of the up-step of the right cavern, the mid-partition wall moves to the right because of the construction deflection pressure caused by tunneling construction between the caverns. A similar phenomenon is also discussed by Duan et al. [35] with regard to a bias-pressure double-arch tunnel, where the bias effect caused by the asymmetric construction is not considered. When the plastic zone of the surrounding rock is initially formed, the primary lining begins to work, and the relative displacement of the cavern gradually moves toward both sides.

- (2) The displacement development pattern of the tunnel cavern is different when subjected to different construction stages. For the first half of the month, because of a rapid stress release of the surrounding rock, the maximum peripheral displacement rate occurs at the early stage, and it moves toward the inner side. Compared with the construction of the lower step, the mid-step construction shows a greater effect on the accumulated displacement and the displacement rate at the UH. The effect of the invert construction on the accumulated periphery displacement and the displacement rate at the UH is greater than the construction of the mid-step. The periphery displacement rate of the left and right caverns converges gradually after the invert construction, which indicates that the timely construction of the invert plays an important role in controlling the displacement of the primary lining and surrounding rock.
- (3) The accumulated peripheral displacement around the UH is larger than the LH because the deflecting retaining wall and the mid-partition wall restrict the horizontal displacement of the lower lining structure and surrounding rock. The accumulated peripheral displacement around the UH is smaller than the LH since there is no deflecting retaining wall on the right side of the right cave, which means that no restraint exists outside the right cave.

4.4. Correlation Analysis

The deformation and stress release of the surrounding rock leads to a settlement in the upper area of the primary lining. According to the test data of the sinking rate of the vault settlement and the steel arch strain, the correlation characteristics between the vault settlement rate and the steel arch strain are explored in Figure 8.

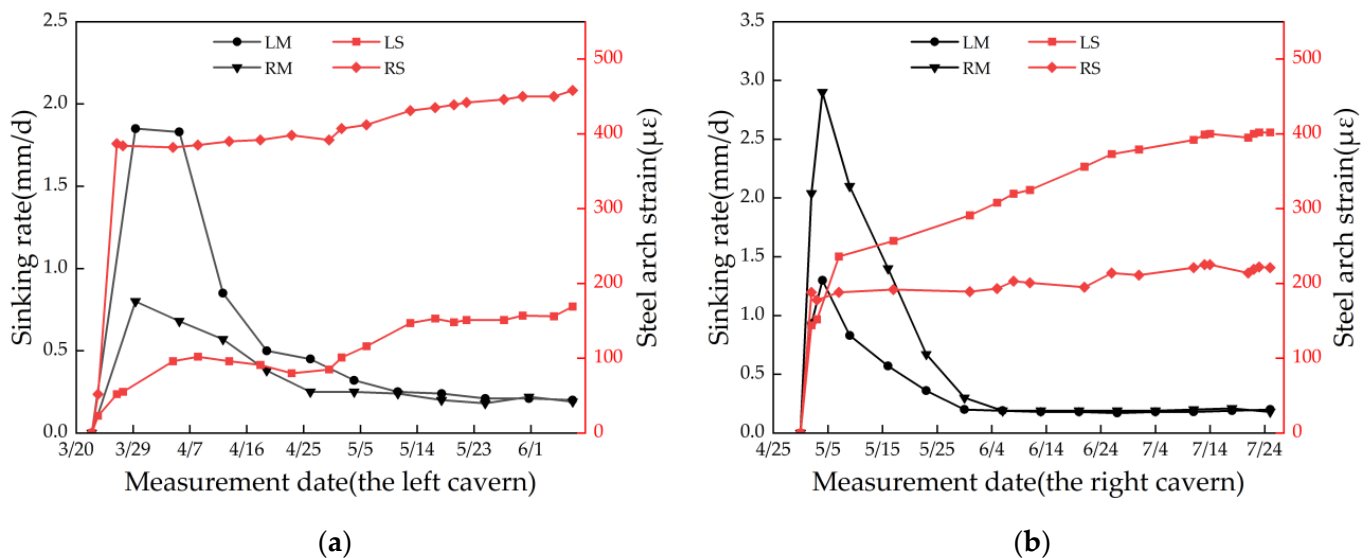


Figure 8. Correlation analysis between the strain and the sinking rate of the primary lining. (a) Left cavern; (b) right cavern.

A rapid development of the vault settlement sinking rate and strain on the steel arch is observed within one week after the erection of the up-step steel arch because the shotcrete does not fully work yet. The surrounding rock pressure is mainly borne by the steel arch. When the shotcrete begins to work, the strength and stiffness of the primary lining are greatly increased, and its proportion for the surrounding rock pressure is also greatly increased. The strain growth rate of the steel arch slows down until stabilization. The supporting function of the steel arch and shotcrete effectively restrains the deformation of the surrounding rock. Thus, the vault settlement rate is greatly reduced. It is seen that (1) the value of the vault settlement rate in the left cavern shows that LM > RM. Additionally,

the strain of the steel arch in the left cave shows that $RS > LS$. (2) The value of the vault settlement rate in the right cavern shows that $RM > LM$, and the strain of the steel arch in the right cavern shows that $LS > RS$.

The reason for the above phenomenon can be concluded as follows. The values of the burial depth at the arch shoulders of each cavern are similar, although the burial depth for the left and right caverns is different (the left cavern is an open cavern where the burial depth of the arch shoulders is 0; the burial depth at the arch shoulders of the right cavern is about 6 m). Without considering any other influencing factors, the values of the surrounding rock pressure on both sides of the caverns are approximately equal. The settlement rate of the vault is related to the surrounding rock pressure. A larger value of the surrounding rock pressure will increase the deformation and settlement rate.

The stress and strain of the steel arch are mainly caused by the surrounding rock pressure. An increasing strain at the steel arch indicates that more surrounding rock pressure is undertaken by the steel arch. The steel arch plays a supporting role and limits the displacement trend and the deformation rate of the surrounding rock.

4.5. Reinforcement Stress of the Secondary Lining

The variation regulation of the reinforcement stress is consistent with that of the concrete strain as for the secondary lining in the open-buried double-arch tunnel. The reinforcement stress of the secondary lining is shown in Figure 9, in which the positive value indicates tension stress and the negative value refers to compressive stress. The initial data derive from the test data when the component is installed.

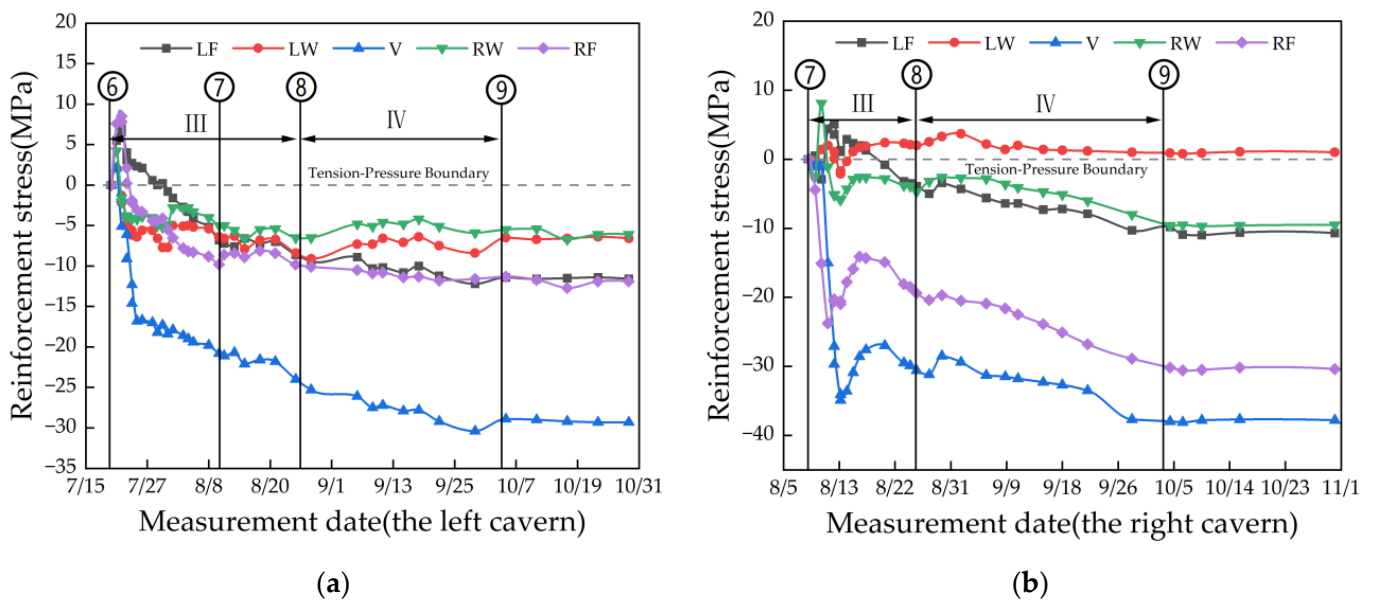


Figure 9. Steel stress of the secondary lining versus time. (a) Left cavern; (b) right cavern.

- (1) The mechanical properties of the reinforcement in the secondary lining are measured throughout the process of concrete casting and maintenance. After the secondary lining concrete is cast in the left and right caverns of the tunnel, the secondary lining forms a temperature gradient from the inside to the outside due to a large amount of heat released from the hydration heat reaction of the concrete. When the concrete cools down and shrinks from a high temperature, this results in tensile stress (temperature stress) [36], causing a significant increase in the tensile stress in the secondary lining. When the maintenance of the secondary lining concrete is completed, it presents a dominated compressive stress.
- (2) Compared with the left cavern, the distribution of stress in the right cavern is more discrete, and a great difference is observed among different measurement points.

The left shoulder of the right cavern is dominated by tensile stress. The supporting effect of the mid-partition wall leads to a relatively concentrated reinforcement stress at the location of the arch waist near the side of the mid-partition wall in the left and right caverns. If the mid-partition wall is taken as a central axis, the value of the reinforcement stress in the left and right caverns can be sorted as follows: vault > outer arch foot > inner arch foot > outer arch waist > inner arch waist. The reinforcement stress at the arch waist of the right cavern is smaller than that in left cavern, while the reinforcement stress at other measurement points of the right cavern is larger than those of the left cavern. Due to the supporting effect of the deflecting retaining wall and the mid-partition wall, the topographic bias will mainly affect the secondary lining of the buried cavern, which effectively controls the bias instability in the open-buried double-arch tunnel.

- (3) Soil backfill presents different effects on the forces of the secondary lining of the left and right caverns. After soil backfill, the surrounding rock pressure above the left cavern increases, which causes the pressure at the V, LF, and RF of the left cavern to increase, especially for the points at the V. The pressure at the LW and the RW of the left cavern shows a decreasing trend. After soil backfill, the vault is firstly subjected to the surrounding rock pressure, which will be transferred to the lower part of the structure (i.e., the arch foot). The inner arch effect produced the waist of the cavern due to a supporting effect from the deflecting retaining wall and the mid-partition wall. Unlike the left cavern, the pressure of the right cavern decreases briefly, and then increases continuously at all measurement points after soil backfill (the soil backfill is above the left cavern), especially for the points at V and RF. The deflecting loading of slope is balanced to some extent after soil backfill above left cavern. A stress adjustment occurs in surrounding rock of right cavern near the right side of slope, and the direction and the size of secondary lining of right cavern change at the same time. When the secondary lining is located at the surrounding rock of right arch foot, the force at the RF and V is most concentrated. At the end of backfilling, the reinforcement stress in the secondary lining of the left and right caverns tends to stabilize and reduce simultaneously, indicating that the interaction between the surrounding rock (including the backfill soil) and the internal linings of the tunnel is gradually balanced and stabilized.

5. Conclusions

To study the mechanical behaviors of the supporting structure and surrounding rock of open-buried multi-arch tunnel, the strain and stress of linings and the deformation laws of the surrounding rock were studied by on-site investigation. The following conclusions are obtained:

- (1) The application of the secondary lining in the left cavern (open cavern) shows an inhibitory effect on the strain development of the steel arch in the right cavern (concealed cavern). The backfill balances the bias caused by the slope and reduces the strain at the steel arch of the concealed cavern.
- (2) The process of vault settlement can be divided into three stages: a rapid development stage within 15 d after the construction of the up-step, the continuous development stage before the application of the invert, and the stable convergence stage after the application of the invert. When the invert is applied, the settlement rate of the vault is gradually stabilized. The mid-partition wall and deflecting retaining wall effectively decrease the settlement of the primary lining and present a weakening effect on the bias effect.
- (3) The peripheral displacement of the tunnel experiences a process of convergence inward and extension outward. The peripheral displacement of the left and right caverns tends to move inward after the construction of the up-step. The deflecting retaining wall and mid-partition wall show a good restraining effect on the tunnel.

Author Contributions: Conceptualization, Y.-L.G. and Y.-L.L.; methodology, Y.-L.G., Y.-L.L., G.-L.Y. and P.-R.Z.; validation, Y.-L.G. and Y.-L.L.; formal analysis, Y.-L.G.; investigation, Y.-L.G. and P.-R.Z.; resources, G.-L.Y.; data curation, Y.-L.G. and Y.-L.L.; writing—original draft preparation, Y.-L.G. and Y.-L.L.; writing—review and editing, Y.-L.L. and Y.-L.G.; visualization, Y.-L.G. and Y.-L.L.; supervision, Y.-L.L. All authors have read and agreed to the published version of the manuscript.

Funding: This research project was funded by the National Natural Science Foundation of China, grant numbers 51878667 and the National Natural Science Foundation of Hunan Province, grant numbers 2021JJ30830.

Institutional Review Board Statement: Not applicable.

Informed Consent Statement: Not applicable.

Data Availability Statement: The data presented in this study may be available on reasonable request from the corresponding author.

Acknowledgments: The authors would like to acknowledge the Civil Engineering Co. Ltd., China Construction Fifth Engineering Bureau for providing detailed information about the design and construction. Meanwhile, the authors would like to express their gratitude to Hong-bo Xiao and Xiong Fu for their help during the field investigation.

Conflicts of Interest: The authors declare no conflict of interest.

References

- Vitali, O.P.M.; Celestino, T.B.; Bobet, A. Analytical Solution for Tunnels Not Aligned with Geostatic Principal Stress Directions. *Tunn. Undergr. Space Technol.* **2018**, *82*, 394–405. [\[CrossRef\]](#)
- Chen, T.; Zhou, K.; Wei, J.; Liu, X.C.; Lin, Y.L.; Zhang, J.; Shen, Q. Analysis on the excavation influence of triangular distribution tunnels for the wind pavilion group of a metro station. *J. Cent. South Univ.* **2020**, *27*, 3852–3874. [\[CrossRef\]](#)
- Yang, C.; Chen, Y.H.; Guo, Z.; Zhu, W.J.; Wang, R.H. Surface Settlement Control in the Excavation of a Shallow Intersection between a Double-Arched Tunnel and a Connection Tunnel. *Int. J. Geomech.* **2021**, *21*, 04021035. [\[CrossRef\]](#)
- Drover, C.; Villaescusa, E.; Onederra, I. Face Destressing Blast Design for Hard Rock Tunnelling at Great Depth. *Tunn. Undergr. Space Technol.* **2018**, *80*, 257–268. [\[CrossRef\]](#)
- Lin, Y.L.; Li, Y.X.; Zhao, L.H.; Yang, T.Y. Investigation on the seismic response of a three-stage soil slope supported by the anchor frame structure. *J. Cent. South Univ.* **2020**, *27*, 1290–1305. [\[CrossRef\]](#)
- Lin, Y.L.; Lu, L.; Yang, G.L. Seismic behavior of a single-form lattice anchoring structure and a combined retaining structure supporting soil slope: A comparison. *Environ. Earth Sci.* **2020**, *79*, 78. [\[CrossRef\]](#)
- Lin, Y.L.; Jin, J.; Jiang, Z.H.; Liu, W.; Liu, H.D.; Li, R.F.; Liu, X. Seismic response of combined retaining structure with inclined rock slope. *Struct. Eng. Mech.* **2022**, *84*, 591–604.
- Huang, X.; Huang, H.; Zhang, D. Centrifuge Modelling of Deep Excavation over Existing Tunnels. *Proc. Inst. Civ. Eng.-Geotech. Eng.* **2014**, *167*, 3–18. [\[CrossRef\]](#)
- Lin, Y.L.; Zhao, L.H.; Yang, T.Y.; Yang, G.L.; Chen, X.B. Investigation on seismic behavior of combined retaining structure with different rock shapes. *Struct. Eng. Mech.* **2020**, *73*, 599–612.
- Lin, Y.L.; Cheng, X.M.; Yang, G.L. Shaking table test and numerical simulation on a combined retaining structure response to earthquake loading. *Soil Dyn. Earthq. Eng.* **2018**, *108*, 29–45. [\[CrossRef\]](#)
- Zhao, C.Y.; Yue, R.H.; Lin, Y.L.; Huang, C.J.; Jiang, X. Investigation on Deformation Behavior of the Crossing Section of two Municipal Road Tunnels during Construction. *Appl. Sci.* **2022**, *12*, 12274. [\[CrossRef\]](#)
- Chang, C.T.; Sun, C.W.; Duann, S.W.; Hwang, R.N. Response of a Taipei Rapid Transit System (TRTS) Tunnel to Adjacent Excavation. *Tunn. Undergr. Space Technol.* **2001**, *16*, 151–158. [\[CrossRef\]](#)
- Sharma, J.S.; Hefny, A.M.; Zhao, J.; Chan, C.W. Effect of Large Excavation on Deformation of Adjacent MRT Tunnels. *Tunn. Undergr. Space Technol.* **2001**, *16*, 93–98. [\[CrossRef\]](#)
- Fahimifar, A.; Tehrani, F.M.; Hedayat, A.; Vakilzadeh, A. Analytical Solution for the Excavation of Circular Tunnels in a Visco-Elastic Burger's Material under Hydrostatic Stress Field. *Tunn. Undergr. Space Technol.* **2010**, *25*, 297–304. [\[CrossRef\]](#)
- Li, S.C.; Yuan, C.; Feng, X.D.; Li, S.C. Mechanical Behaviour of a Large-Span Double-Arch Tunnel. *KSCE J. Civ. Eng.* **2016**, *20*, 2737–2745. [\[CrossRef\]](#)
- Liu, X.; Sun, Q.H.; Song, W.; Bao, Y.H. Structural Behavior of Reinforced Concrete Tunnel Linings with Synthetic Fibers Addition. *Tunn. Undergr. Space Technol.* **2023**, *131*, 104771. [\[CrossRef\]](#)
- Xue, Y.G.; Gong, H.M.; Kong, F.M.; Yang, W.M.; Qiu, D.H.; Zhou, B.H. Stability Analysis and Optimization of Excavation Method of Double-Arch Tunnel with an Extra-Large Span Based on Numerical Investigation. *Front. Struct. Civ. Eng.* **2021**, *15*, 136–146. [\[CrossRef\]](#)
- Li, N.N.; Zhou, Y.Q.; Zhao, Y.Q.; Li, G.J. Analysis of Mechanical Behavior of Double Arch Tunnel by CD Method and Benching Method. *IOP Conf. Ser. Earth Environ. Sci.* **2020**, *580*, 012074. [\[CrossRef\]](#)

19. Barla, G. Full-Face Excavation of Large Tunnels in Difficult Conditions. *J. Rock Mech. Geotech. Eng.* **2016**, *8*, 294–303. [[CrossRef](#)]
20. Rehman, H.; Naji, A.M.; Ali, W.; Junaid, M.; Abdullah, R.A.; Yoo, H. Numerical Evaluation of New Austrian Tunneling Method Excavation Sequences: A Case Study. *Int. J. Min. Sci. Technol.* **2020**, *30*, 381–386. [[CrossRef](#)]
21. Lee, J.K.; Yoo, H.; Ban, H.; Park, W.-J. Estimation of Rock Load of Multi-Arch Tunnel with Cracks Using Stress Variable Method. *Appl. Sci.* **2020**, *10*, 3285. [[CrossRef](#)]
22. Dong, J.S. Study on the Soil Structure and Construction Technology of Large Span Double-Arch Tunnel Entrance. *IOP Conf. Ser. Earth Environ. Sci.* **2021**, *804*, 022080. [[CrossRef](#)]
23. Cai, J. Determination of the Installation Time of Secondary Liner during Excavation of Large Cross-Section Double-Arch Tunnels. *Adv. Civ. Eng.* **2020**, *2020*, 8852181. [[CrossRef](#)]
24. Li, C.L.; Wang, S.R.; Wang, Y.G.; Cui, F.; Yang, F. Skewed Pressure Characteristics of Equivalent Load in Double-Arch Tunnel. *J. Eng. Technol. Sci.* **2016**, *48*, 345–358. [[CrossRef](#)]
25. Li, X.C.; Yang, S.; Dai, R.; Ai, Z.B.; Zhang, C.; Huang, X. Analytical Solutions for the Internal Forces of Lining Structure in Shallow Double-Arched Tunnel Subject to Unsymmetrical Loads. *Earth Environ. Sci.* **2020**, *570*, 052029. [[CrossRef](#)]
26. Sui, Y.; Cheng, X.H.; Wei, J.X. Distributed Fibre Optic Monitoring of Damaged Lining in Double-Arch Tunnel and Analysis of Its Deformation Mode. *Tunn. Undergr. Space Technol.* **2021**, *110*, 103812. [[CrossRef](#)]
27. Shi, C.H.; Peng, L.M. Study on construction method of double-arch tunnel with half-open and half-hidden structure. *Chin. J. Rock Mech. Eng.* **2007**, *26*, 2809–2814.
28. Lai, J.X. Design of partially buried double-arch tunnel with super-large span (2×4 lanes). *Mod. Tunn. Technol.* **2007**, *44*, 30–35.
29. Hu, H.B.; Yang, J.S.; Yang, F. Selection of “half-lit and half-dark” or “half-road and half-tunnel” structure types for continuous arch tunnels under skewed terrain conditions. *Mod. Tunn. Technol.* **2008**, *45*, 283–288.
30. Guo, J.; Yang, J.S.; Chen, W.; Shen, D.; Liu, T.; Cai, W.Y. Research on large deformation of surrounding rock and mechanical characteristics of lining of carbonaceous slate tunnel based on field measurement. *Chin. J. Rock Mech. Eng.* **2019**, *38*, 832–841.
31. Zhao, Y.; Liu, J.Y.; Tian, S.M. Experimental Study of Mechanical Characteristics of Support System for Weak Surrounding Rock of Deep Tunnels. *Chin. J. Rock Mech. Eng.* **2011**, *30*, 1663–1670.
32. Zhou, D.H.; Cao, L.Q.; Wang, X.X.; Fang, S.T. In-situ tests on lining system of double-arch tunnel with shallow large section and span. *Chin. J. Geotech. Eng.* **2010**, *32*, 1573–1581.
33. Wang, W.Z.; Liang, Q.G.; Jia, G.Y.; Shi, B.D. Statistical Analysis of the Contact Pressure between the Primary Support and the Secondary Lining of Tunnel. *Chin. J. Undergr. Space Eng.* **2021**, *17*, 1586–1597.
34. Yuan, Y.; Wang, S.H.; Du, G.P.; Li, D. In-Situ Testing Study on Lining System of Double-Arched Tunnel. *Chin. J. Rock Mech. Eng.* **2005**, *24*, 480–484.
35. Duan, H.P.; Xu, G.C.; Liu, B.G. Analysis of Deformation of Surrounding Rock and Stress Characteristics of Supporting Structure of FUXI Twin Tunnel. *Chin. J. Rock Mech. Eng.* **2006**, *25*, 3763–3768.
36. Zhang, C.Q.; Guo, X.H.; Tian, L.D.; Zhang, P.; Chen, J.; Huang, Y.X.; Wang, C.K.; Zheng, B.Y. Influence of Restraint on Distribution of Early Thermal Stress of Tunnel Secondary Lining. *Tunn. Construct.* **2017**, *37*, 67–71.

Disclaimer/Publisher’s Note: The statements, opinions and data contained in all publications are solely those of the individual author(s) and contributor(s) and not of MDPI and/or the editor(s). MDPI and/or the editor(s) disclaim responsibility for any injury to people or property resulting from any ideas, methods, instructions or products referred to in the content.